Correlating cation coordination, stiffness, phase transition pressures, and smart materials behavior in metal phosphates

Dmitry Shakhvorostov and Martin H. Müser
Department of Applied Mathematics, University of Western Ontario, London, ON, Canada, N6A 5B7

Nicholas J. Mosey
Department of Chemistry, Queen's University, Kingston, ON, Canada K7L 3N6

Yang Song and Peter Norton
Department of Chemistry, University of Western Ontario, London, ON, Canada N6A 5B7
(Dated: November 7, 2008)

In this study, we present X-ray diffraction data on zinc- and calcium phosphates. The experiments reveal that low-coordinated zinc phosphates are relatively soft at ambient conditions but stiffen dramatically with pressure, p, exhibiting smart materials behavior, while high-coordinated zinc and calcium phosphates have higher initial bulk moduli and stiffen considerably less rapidly with increasing p. All systems amorphize when their bulk modulus reaches a value near 210 ± 40 GPa, where the precise value depends on chemical details, indicating that phosphate networks become unstable when their bulk modulus reaches that value. Our ab initio simulations of zinc α-phosphate support the idea that the elastic properties are controlled by the motion of rigid phosphate units, which becomes more hindered under densification, with or without increasing cation coordination. It is discussed how these results may explain why low-coordinated zinc phosphates are good anti-wear agents.

PACS numbers: Valid PACS appear here

I. INTRODUCTION

The mechanical properties of metal phosphates are of interest in science and engineering, in particular for their stress-history dependence. The stress-history dependence was found, for instance, in various heavy-metal phosphates indicative of meta-stable phases[1,2]. One of the examples is lead phosphate - a paramount ferroelastic and thus also stress-history dependent[3,4]. Zinc phosphates (ZP), for instance, are used in dental restoration as an important component of cements[5] as well as calcium phosphates (CP), which have considerable biological importance with respect to the biomineralization processes in bones and teeth[6]. Hydrogenated calcium phosphates are potential candidates for application as protonic conductors[7]. But despite the applications described above, probably the technologically most relevant application of the phosphates is in their use as various additives in lubricated systems[8]. Zinc phosphates and calcium phosphates form a significant part of the protective film formed on surfaces during friction in a lubricated engine. The stress-history of the film is of particular interest to gain understanding of its protective nature.

A microscopic mechanism for the stress-history dependence of metal phosphates was suggested previously on the basis of first-principles molecular dynamics simulations in which systems composed of loosely-connected ZP molecules were subjected to time-dependent external pressures[9]. The results demonstrated that zinc, which was tetra-coordinate and tetrahedral in the initial structure at ambient pressures (although it fluctuated between di-, tri- and tetra-coordinate states in some simulations) adopted a tetra-coordinate 'see-saw' geometry when compressed to 6 GPa. The additional coordination sites available at the zinc atom in this configuration led to the formation of bonds between zinc and oxygen atoms in neighboring phosphate chains. The formation of these bonds increased the degree of connectivity between the phosphate chains in the system, with zinc acting as the network-forming agent. Upon decompression to ambient pressures, the zinc atom reverted to a tetra-coordinate state; however, the Zn-O bonds associated with the increased connectivity in the system persisted. It was argued that this irreversible transformation of loosely-connected ZPs into a highly-connected ZP network, and the concomitant effects on the mechanical properties of the system, play an important role in the formation and functionality of ZP antiwear films[10].

To test the theoretical hypothesis, two experimental studies of the stress-history of various hydrogenated and nonhydrogenated zinc and calcium phosphates were conducted using X-ray absorption techniques and vibrational spectroscopy[11,12]. The most important result of these studies is that zinc phosphates amorphize under compression and yield at distinctly lower pressures than calcium phosphates or pure phosphates, and hydrogenated metal phosphates yield earlier than nonhydrogenated metal phosphates. It was argued that the low pressure, at which the orthophosphate of zinc amorphizes, can be explained with its ability to change coordination. An orbital analysis revealed that zinc can bind on to additional oxygen atoms by hybridizing a d orbital with a p orbital of a bridging oxygen into a σ bond. It was pointed out that hydrogen terminated pure phosphates yield at

even higher pressures than hydrogen-free calcium phosphates. In the case of pure phosphates, the coordination number changed on some of the phosphorus atoms from four to five upon compression. This was followed by the conclusion that the phosphate unit itself is stable up to pressures of 26 GPa and that the disordering in the calcium phosphates must be due to changes associated with the cation.

In the studies on metal phosphates under pressures, some critical questions remain unanswered. In the previous publications on the stress history of calcium and zinc phosphates, it was not investigated whether the triggering mechanism of loss of crystallinity is connected to the cation site, and how the critical pressures depend on the initial coordination of the cation sites. No refinement of the crystal structure to obtain the equations of state have been made so far, to study either the stiffening or the bulk modulus of zinc and calcium phosphates up to pressures of 25 GPa. In particular, it remains unanswered how the connectivity of the phosphate anions through the cation sites would affect the bulk modulus. It is the purpose of this article to address these open issues. To answer the above mentioned questions, we have performed experiments in which the phosphates were exposed to isotropic pressures and their structure was *in situ* investigated by X-ray diffraction using synchrotron radiation. The systems used in the experiments are as follows: α-$Zn_3(PO_4)_2$, pyrophosphate $Zn_2P_2O_7{\cdot}H_2O$, $Zn(H_2PO_4)_2$ and for comparison of different cation types we used β-$Ca_3(PO_4)_2$ and α-$CaHPO_4$. Experiments using calcium phosphates were also performed to investigate the effect of replacing zinc, while hydrogenated zinc- and calcium-phosphates were used to study the influence of hydrogen on any observed processes. In addition, a first-principles calculation was performed to complement the experiments on α-$Zn_3(PO_4)_2$.

In addition to the questions raised in the previous paragraph, one can ask what the microscopic origin of the "smart materials" behavior observed in zinc phosphate containing anti wear films may be[13]. Materials are called smart when they adapt their response to an external stimulus in an unusually strong fashion, e.g., if their bulk modulus K increases with pressure p not simply by a value in the order of the applied pressure but by a large multiple of p (i.e., if $dK/dp \gg 1$). Values of dK/dp for regular metals and semiconductors are near five[14–18]. In the theory for the functionality of anti-wear agents[9], it had been argued that the stiffening observed in zinc phosphates can be explained with a change of coordination on zinc. However, inspection of numerical data on simple phosphates and zinc phosphates shown in Ref. 19 (Figs. 1 and 2), is suggestive of strong stiffening even without coordination change on the cation. Thus, it remains to be answered if there are competing explanations for the stiffening in zinc phosphates.

The remainder of this article will be organized as follows. In section II, we describe experimental and computational methods. Section III contains the results from high pressure X-ray diffraction experiments using synchrotron radiation as well as numerical results in addition to those presented in Ref. 9 or Ref. 12. Conclusions are drawn in section IV.

II. METHODS

A. Experimental details

In this study, samples are exposed to isotropic stresses and their structure is characterized *in situ* by X-ray diffraction (XRD) using synchrotron radiation. The following sections describe the details of the high pressure equipment, sample preparation, as well as the experimental setup of XRD experiment.

1. High pressure equipment

For sample compression, a symmetric piston-cylinder type of diamond anvil cell (DAC) equipped with 400 μm culet diamond anvils was used. A few ruby (Cr^{+3} doped α-Al_2O_3) chips as pressure calibrant, were carefully placed inside the gasket sample chamber before the sample was loaded. The pressure was determined from the well known pressure shift of the R_1 ruby fluorescence line (at 694.2 nm under ambient conditions) with an accuracy of $\pm$ 0.05 GPa under quasi-hydrostatic conditions[20]. A custom made Raman spectrometer was used for pressure determination. The latter was calibrated at several absorption lines using diamond and silicone standards to ensure linearity of the wave number scale. Purity of all phosphates obtained from Aldrich is 99.999% except $Zn(H_2PO_4)_2$, which was prepared as described in Ref. 21. The structure of the latter was verified using X-ray diffraction. The samples were loaded at room temperature and relative humidity of 60 - 80% as powder with nominal pressure slightly above ambient using silicon oil as a pressure transmitting medium. Then the cell is carefully pressurized with small steps and allowed to stabilize for a few minutes after each pressure change before Raman spectra were taken. Experiments were conducted up to 25 GPa and reproduced a few times, except for the $Zn(H_2PO_4)_2$ that was investigated up to a maximum pressure of 7 GPa.

2. X-ray diffraction (XRD) of synchrotron radiation

X-ray diffraction (XRD) was used to identify reversible changes induced by pressure increase as well as to validate our assumptions on the initial structure of the zinc and calcium phosphate used in experiments. X-ray diffraction spectra (at 30.55 keV; λ = 0.4066 nm) were collected under isotropic compression at the X17C beam line of the National Synchrotron Light Source at

Brookhaven National Laboratory. To collect the spectra a CCD camera was used and the exposure time was set equal for all experiments to 400 s. The data were integrated using the Fit2D software and data analysis software such as POWDERCELL.

B. Simulation details

First-principles molecular dynamics (MD) simulations of α-$Zn_3(PO_4)_2$ were performed to complement the experiments. The simulated structures were then used to calculate XRD spectra in order to compare them with the experimental ones for refinement of the coordination on the cation site. The simulations were performed on a single unit cell of α-$Zn_3(PO_4)_2$ and periodic boundary conditions were employed to treat this system as a bulk material. The α-ZPs were compressed/decompressed by applying isotropic, time-dependent pressures and allowing the size and shape of the simulation cell to vary in response to the changes in pressure. This procedure ultimately applies the pressure to the atoms in the system, thereby permitting pressure-induced chemical reactions.

The specific details associated with the (de)compression of the system are as follows. First, the system was equilibrated at a temperature of 300 K and a pressure of 0.0 GPa. The external pressure was then increased linearly at a rate of 10.0 GPa/ps until a maximum pressure of $P_{\max} = 15$ GPa was reached. The pressure was then decreased at the same rate until a final pressure of 0.0 GPa was attained. Overall, this procedure mimics the changes in pressure experienced in the experiments, where the ZPs are compressed/decompressed over a range of pressures spanning several GPa. However, it is important to note that the rate of (de)compression employed in the simulations is significantly higher than that used in the experiments, which will likely preclude thermal activation in the simulations. Hence, the pressures required to induce processes in the simulations upon compression will be higher, and upon decompression, will be lower than those required to induce similar processes in the experiments.

The simulations were performed within the Car-Parrinello MD extended Lagrangian formalism[22] with the CPMD software package,[23] which we modified to allow the applied pressure to vary with time. The electronic structure was solved using Kohn-Sham density functional theory[24] with the exchange-correlation functional of Perdew, Burke and Ernzerhof.[25] The valence electrons were represented by a set of plane-waves expanded at the Γ-point up to a kinetic energy cutoff of 120 Ry and the core elecrons were represented with norm-conserving pseudopotentials.[26] Tests on ZPs indicate that this simulation methodology yields pressures that agree to within 0.2 GPa of those obtained with a plane wave cutoff of 200 Ry. The nuclear coordinates were propagated using a time step of 2.0 a.u. and the fictitious electron mass was set at 400 a.u. This conserved the total energy of the system to better than 10^{-5} a.u./ps.

III. RESULTS

In this section we present the results of high pressure behavior of zinc and calcium phosphates. Each subsection gives information about structural details of the specific compound and details of the cation environment therein. Our computational results on α-$Zn_3(PO_4)_2$ are reported within the experimental section for direct comparison.

A. Zinc phosphates

1. *Zinc orthophosphate α-$Zn_3(PO_4)_2$*

Prior to the high pressure experiments, we verified the crystal structure of the zinc orthophosphate using X-ray diffraction and Raman spectroscopy at ambient conditions. Both confirmed that anhydrous zinc α-orthophosphate can be described in the monoclinic space group $C2/c$ with lattice parameters $a = 8.14 \pm 0.02$ Å, $b = 5.63 \pm 0.01$ Å, $c = 15.04 \pm 0.04$ Å, $\beta = 105°08' \pm 05'$, and $Z = 4$[27]. In this structure, the zinc cations have two types of tetrahedrally coordinated sites. One-third of the cations lies on twofold axes within an oxygen tetrahedron. The remaining cations are located in a pair of edge-sharing oxygen atom tetrahedra.

Upon compression, X-ray reflections broaden and slightly shift to higher angles with respect to those at ambient pressure, see Fig. 1. However, the initial crystal structure remains stable up to about 5 GPa, In the pressure region between 5.7 GPa and 13.8 GPa, the (110) and (-111) reflections are suppressed and the reflections (-113) and (114) shift at higher rates than the remaining reflections, which is indicative of a modified structure. The reflections weaken so significantly that it is safe to assume disordering in the system, in particular as the vanished reflections represent long-range order. In the following, we will refer to this structure as "intermittent phase" (IP).

When we decompress samples that had not been exposed to pressures beyond 5 GPa, the initial crystalline structure recovers to a significant degree. If, however, samples have been exposed to pressures above 7 GPa, no signs of the long wavelength reflections reoccur, indicating an irreversible loss of crystallinity, supporting our conclusions from a previous Raman experiment[12], in which we argued that zinc α-orthophosphate amorphizes at approximately 7 GPa.

Upon further compression, new peaks appear at small angles as shown in the XRD pattern (Fig. 1) beyond pressures of 13.8 GPa, indicating the formation of a new high-pressure (HP) phase. The HP phase could be indexed in

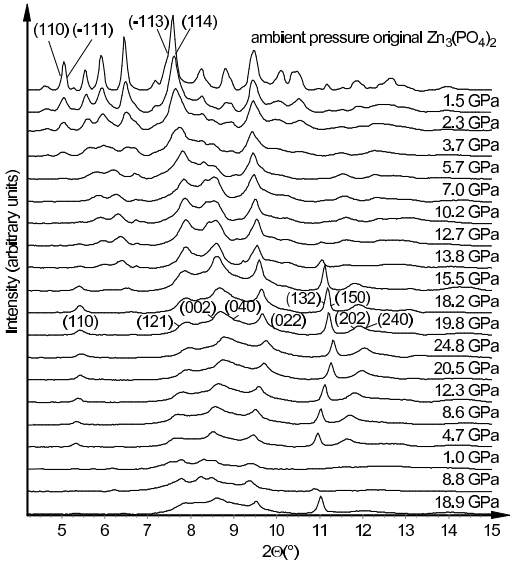

FIG. 1: X-ray diffraction spectra of α-$Zn_3(PO_4)_2$ during a compression/decompression cycle.

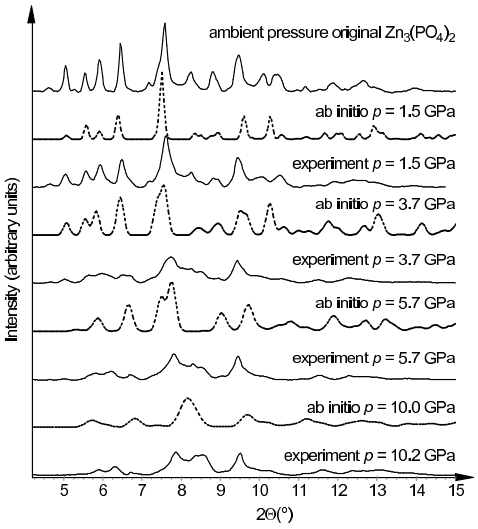

FIG. 2: Comparison of the experimentally measured and the calculated *ab initio* X-ray diffraction spectra for α-$Zn_3(PO_4)_2$ during compression.

the orthorhombic space group $Iba2$ with the unit cell parameters of $a = 4.71$, $b = 10.79$, $c = 5.43$, $(Z = 2)$. The new structure contains two molecules in the elementary cell instead of four as in the original structure and moreover, the HP structure has higher symmetry. As a note of caution we want to emphasize that the identification of the cell dimensions and space group is based on broad experimental peaks, which leaves the possibility of alternative space groups, superstructure, etc.

In order to gain more insight into the detailed atomic structure of zinc α-phosphate under pressure, we run *ab initio* simulation of that material and calculated the spectra, which would have been produced by the computed geometries. The comparison between experimental and numerical X-ray data is shown in Fig. 2. We find very good agreement in the pressure region from 0 to 3.7 GPa, i.e., as long as the unit cell is seen to be stable experimentally. At higher pressures, in particular beyond 5.5 GPa, one cannot expect similarly good agreement due to the small size of the simulation cell, which accommodates only a single unit cell of zinc α-phosphate. Nonetheless, it seems as though the experimental spectra at 5.7 GPa can be described as a superposition of the calculated spectra from the 5.7 and 10.0 GPa simulations. This indicates that the local in the experiment at 5.7 GPa is a mixture of the local orders described in the simulations at 5.7 and 10.0 GPa.

Investigation of the local structures reveals the nature of the transition between low- and high-pressure coordination as found in the simulations. For this purpose, two molecules of α-$Zn_3(PO_4)_2$ are depicted in Fig. 3 under ambient pressure and during compression at 10 GPa. It can be seen that there are phosphate tetrahedra that rotate in a rigid-mode type fashion, such that the coordination on a third of the zinc atoms increases from four to five. The process occurs at 9 GPa and reverts upon decompression at 4 GPa. Further compression to ≈ 13 GPa induces an additional increase of the coordination from five to six, again via rigid mode-type rotations of tetrahedral units. At presures above 9 GPa, the remaining Zn cations assume a see-saw geometry. For reasons outlined further below, we associate the five- and six-coordinated structures with the local order in the experimental IP and HP phase, respectively.

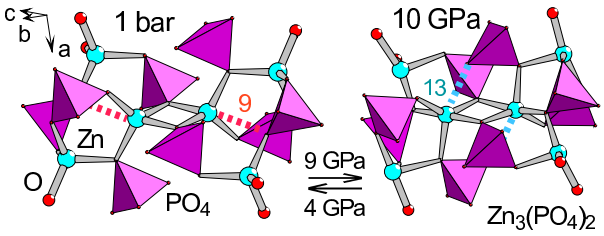

FIG. 3: (Color online.) Structural changes in α-$Zn_3(PO_4)_2$ during a compression/decompression cycle. The left and right graph show a configuration of two α-$Zn_3(PO_4)_2$ molecules at $p = 1$ bar and 10 GPa, respectively. Zn and O atoms are indicated explictly in the figure, while P atoms are in the center of the tetrahedra. Colored dotted lines indicate bonds that will be formed upon compression. Numbers nearby these bonds show their formation pressures in units of GPa. One third of Zn cations changes their coordination from 4 to 5 upon compression at approximately 9 GPa, and revert at 5 GPa. The remaining Zn cations assume a see-saw configuration in the intermittent-phase (9 GPa $\leq$ p $\leq$ 13 GPa). Upon compression to approximately 13 GPa the pentacoordinated Zn cations assume sightly distorted octahedral configuration. The dotted blue lines show the bonds that will appear in that phase.

The refinement of the unit cell geometry using the experimental data allowed us to construct an equation of

state up to the pressure of 5.7 GPa, see Fig. 4. Further compression disturbed the structure to the extent that no accurate refinement could be processed with the use of a single crystal symmetry so that no volume-pressure relation can be extracted from X-ray. Beyond 13.8 GPa, the equation of state can be calculated again by making use of the proposed high pressure symmetry. In this phase, as well as in the low-pressure, the agreement between measured and simulated density is essentially flawless. This observation gives us further confidence that the local order in the HP structures are similar in experiment and simulation. Moreover, simulation and experiment indicate an instability of the initial unit cell geometry in the same pressure region between 4 and 5 GPa. The simulation shows a second instability at a pressure around 9 to 10 GPa, which correlates with the coordination increase at one third of the cations from four to five. The HP phase remained stable in both simulation and experiment to the maximum applied pressures of 15 and 25 GPa, respectively.

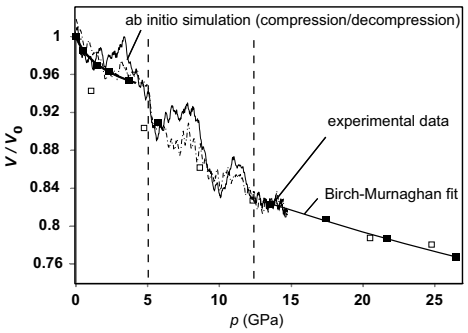

FIG. 4: Equation of state as obtained from our X-ray diffraction experiments and *ab initio* simulation. Dashed lines indicate pressures of structural transformations during compression of α-$Zn_3(PO_4)_2$. Rectangles show the experimental data, which is fitted using Birch-Murnaghan[28] relation, which we use to obtain the bulk modulus. Bulk modulus $K(0) = 36.2 \pm 4.3$ GPa, $K'(0) = 15.3 \pm 5.1$.

The bulk modulus and its pressure dependence can be determined from a Birch-Murnaghan[28] fit via the equation $K(p) = -\partial \ln V/\partial p$, as long as the fit represents the experimentally measured curve sufficiently well. At ambient pressure, we obtain a bulk modulus of $K(0) = 36.2 \pm 4.3$ GPa, and a pressure derivative, $K'(0) = 15.3 \pm 5.1$. This compares very well to the data obtained from the simulations, which is $K(0) = 49 \pm 3.2$ GPa and $K'(0) = 10.9 \pm 6.3$. Thus, we have observed the smart materials effect mentioned in the introduction within a single phase and without a change of cation coordination.

Analysis of the bulk modulus of the low-pressure phase as a function of pressure reveals that $K(p)$ increases quite dramatically in an almost linear fashion with p up to a value of 190 GPa at the instability point. In the disordered phase, it is difficult to ascertain $K(p)$ from both experiment and simulation, because (a) the disordered nature of the IP prohibits a meaningful indexing, and (b) the short time spans in the simulations combined with strong hysteresis effects in the IP make it impossible to disentangle latent volume effects due to the transition and true changes in compressibility. The HP phase has a much weaker pressure dependence than the low-pressure phase. Its bulk modulus only increases from 200 to 220 GPa, when p is increased from 13 GPa to 25 GPa so that dK/dp is only 3% with respect to that of the low-pressure phase. We believe that these findings are significant for the explanation of why low-coordinated zinc phosphates perform well as antiwear agents, which will be discussed in the conclusions section.

2. *Hydrogenated zinc orthophosphate $Zn(H_2PO_4)_2$*

In order to study the effect of the hydrogenation on the stress history of the zinc phosphates we used a synthesized $Zn(H_2PO_4)_2$ as described in Ref. 21, whose structure has been verified at ambient conditions using X-ray diffraction (XRD)[21] and infrared (IR) spectroscopy. To our knowledge there is no commercially available hydrogenated zinc phosphate with a refined atomistic structure, which is why we were limited to the use of a synthesized compound with an unknown atomic structure. Our experimental data as well as data published in Ref. 21 indicate that the structure of the $Zn(H_2PO_4)_2$ can be modeled in the space group $P2_1/c$ (14) with unit cell dimensions $a = 5.336 \pm 0.05$ Å, $b = 9.85 \pm 0.1$ Å, $c = 8.599 \pm 0.1$ Å, $\beta = 122.42°$. The zinc cation coordination in the orthophosphates as well as in ZnO and ZnSe is usually equal to four[29], which we assume to be the most probable coordination number in the given compound; however to gain more certainty about the local environment of the cation in the hydrogenated zinc phosphate, its structure has to be solved from a single crystal.

The compression protocol for the $Zn(H_2PO_4)_2$ was similar to the one for α-$Zn_3(PO_4)_2$, however at the time of the experiment, the maximum studied pressure of interest was limited to 7 GPa. After compression to this pressure, the structure of the $Zn(H_2PO_4)_2$ was irreversibly distorted. The results of the compression are shown in the form of an equation of state as obtained from X-ray diffraction (see Fig. 5). The equation of state indicates a transition at about 3 GPa. The crystal distorts to a significantly lower degree than α-$Zn_3(PO_4)_2$. This allows us to determine the equation of state even in the distorted phase by using the original crystal geometry. The bulk modulus obtained from the equation of state and the Birch-Murnaghan fit, and its pressure derivative at ambient pressure are $K(0) = 15.1 \pm 2.0$ GPa, $K'(0) = 67.5 \pm 20$ respectively. After the transition, the values increase to $K(3.5) = 125 \pm 5$ GPa, $K'(3.5) = 45 \pm 10$.

For this low-coordinated zinc phosphate, we also observe a dramatic increase of the bulk modulus with pressure, specifically an increase from 15 GPa at ambient to

≈ 200 GPa at 3 GPa. The bulk modulus increases again rather quickly in the new phase from 125 GPa at 3 GPa to 220 GPa at 7 GPa.

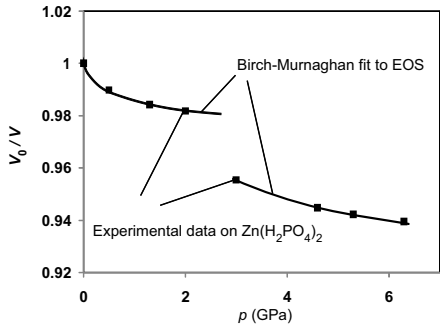

FIG. 5: Equation of state as obtained from our X-ray diffraction experiments. Rectangles show the experimental data, which is fitted using Birch-Murnaghan[28] relation to obtain the bulk modulus and its pressure derivative at ambient pressure. Bulk modulus $K(0) = 15.1 \pm 2.0$ GPa, $K'(0) = 63.5 \pm 20$. The dashed line indicates onset of the amorphization during compression of $Zn(H_2PO_4)_2$.

3. *Zinc pyrophosphate monohydrate $Zn_2P_2O_7{\cdot}H_2O$*

A high coordination of zinc cation can be found in α-$Zn_2P_2O_7$ that has monoclinic symmetry with unit cell parameters $a = 20.068$, $b = 8.259$, $c = 9.099$, $\beta = 106°35'$, and $Z = 12$, and the space group $I2/c$. As commercially available α-$Zn_2P_2O_7$ is hygroscopic it easily transforms in the atmosphere to the $Zn_2P_2O_7{\cdot}H_2O$[30] structure. The latter can be refined using the Rietveld method with dimensions of the unit cell $a = 19.05 \pm 0.05$ Å, $b = 8.07 \pm 0.1$ Å, $c = 9.23 \pm 0.1$ Å, $\beta = 106°35' \pm 05'$. The hydration of the α-$Zn_2P_2O_7$ does not affect the symmetry of the pyrophosphate ($I2/c$), which in the original structure has one third of the cations with a coordination number of 6, and the rest with coordination 5[31]. The average coordination of the zinc cation is therefore 5.33.

From the equation of state (Fig. 6), as obtained from X-ray diffraction experiments, it can be seen that the original crystalline structure remains stable upon compression up to 17 GPa. At pressures higher than 17 GPa, the structure is distorted making it difficult to refine the cell size. The last point in the figure was determined using only the high angle (small d-spacings) reflections and thus might not be very precise. The distorted crystalline order remains upon decompression. The irreversible amorphization of the pyrophosphate was also reported earlier[11].

From the equation of state the bulk modulus and its pressure dependence can be determined using Birch-Murnaghan fit, which reveals that the bulk modulus increases from $K(0) = 81.5 \pm 1.5$ GPa at an almost constant rate ($K'(0) = 5 \pm 0.5$). This is a much weaker pressure dependence than the one of low-coordinated zinc phosphates.

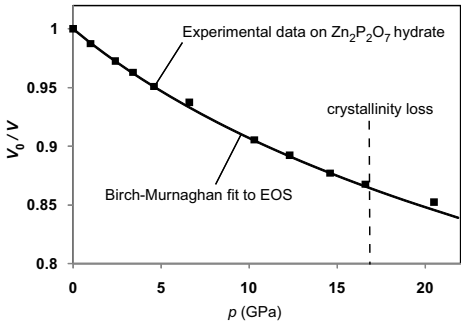

FIG. 6: Equation of state as obtained from our X-ray diffraction experiments. Rectangles show the experimental data, which is fitted using Birch-Murnaghan[28] relation to obtain the bulk modulus and its pressure derivative at ambient pressure. Bulk modulus $K(0) = 81.5 \pm 1.5$ GPa, $K'(0) = 5 \pm 0.5$. The dashed line indicates onset of the amorphization during compression of $Zn_2P_2O_7{\cdot}H_2O$.

B. Calcium phosphates

1. *Synthetic monetite, $CaHPO_4$*

The crystal structure of $CaHPO_4$ was confirmed by XRD and can be described in the triclinic setting (space group $P1$) with unit cell parameters $a = 6.90$ Å, $b = 6.65$ Å, $c = 7.00$ Å, $\alpha = 96.4°$, $\beta = 103.9°$, $\gamma = 88.7°$ and $Z = 4$[32,33]. Calcium has two independent Ca sites with the coordination numbers 7 and 8 respectively, resulting in an average coordination number of 7.5. The equation of state as obtained from XRD measurements indicates no crystal-crystal transition up to a pressure of 18 GPa (see Fig. 7). The bulk modulus increases from $K(0) = 33.4 \pm 5.0$ GPa at a relatively modest rate ($K'(0) = 21.5 \pm 5.1$).

2. *β-tricalcium phosphate $Ca_3(PO_4)_2$*

Using XRD we confirmed that β-$Ca_3(PO_4)_2$ has the space group $R3c$, $Z = 21$ with unit-cell parameters $a = b = 10.4352$ Å, $c = 37.4029$ Å, $\alpha = \beta = 90°$, $\gamma = 120°$ in the hexagonal setting, where positional parameters for oxygen with equal precision were obtained previously by the neutron powder diffraction technique[34]. The coordination of the calcium cations in β-$Ca_3(PO_4)_2$ varies from three to eight. One cation site is very different from the other four sites. It is three-fold coordinated with oxygen atoms, and has a low occupancy factor of 0.43. By contrast, each of the other four cation sites is fully occupied by one calcium atom, and these positions are coordinated with seven, eight, eight, and six oxygen atoms, respectively. The average coordination num-

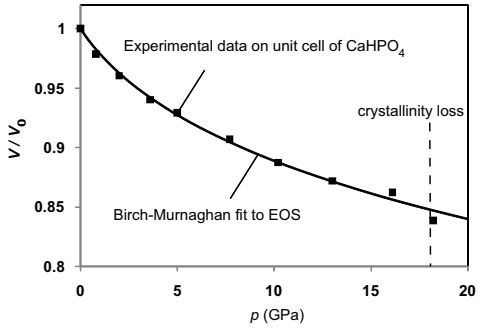

FIG. 7: Equation of state as obtained from our X-ray diffraction experiments. Rectangles show the experimental data, which is fitted using Birch-Murnaghan[28] relation to obtain the bulk modulus and its pressure derivative at ambient pressure. Bulk modulus $K(0) = 33.4 \pm 5.0$ GPa, $K'(0) = 21.5 \pm 5.1$. The dashed line indicates onset of the amorphization during compression of $CaHPO_4$.

ber is therefore 6.7. The equation of state as obtained from XRD measurements is shown in Fig. 8. There is no indication of a phase change up to a pressure of 21 GPa where the calcium phosphate structure becomes distorted. The bulk modulus increases from ambient values $K(0) = 96.7 \pm 4.9$ GPa at a rate of $K'(0) = 7.4 \pm 1.0$ to the maximum value again in a nearly linear fashion.

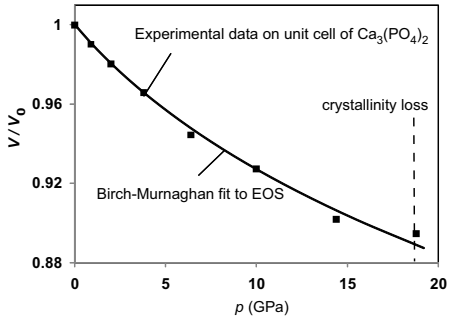

FIG. 8: Equation of state as obtained from our X-ray diffraction experiments. Rectangles show the experimental data, which is fitted using Birch-Murnaghan[28] relation to obtain the bulk modulus and its pressure derivative at ambient pressure. Bulk modulus $K(0) = 96.7 \pm 4.9$ GPa, $K'(0) = 7.4 \pm 1.0$. The dashed line indicates onset of the amorphization during compression of β-$Ca_3(PO_4)_2$.

IV. CONCLUSIONS

In this section we will discuss our experimental results from two points of view. First we wish to rationalize the transition history of calcium and zinc phosphates in the quest for a universal mechanism for pressure-induced phase transitions of simple metal phosphates. Second, we would like to discuss possible implications of our results to tribology.

A. Solid state chemistry

In our experiments, we observe the following trend: metal phosphates with low coordination are relatively compliant at ambient conditions. However, they stiffen rapidly under increasing pressure, p, and their original crystalline structures become thermodynamically unstable at relatively small p, at which point they amorphize. In contrast, crystalline metal phosphates with high cation coordination are relatively stiff at ambient conditions and stiffen with low rates as p increases. They amorphize at higher pressures than the low-coordinated metal phosphates. These results are summarized in Fig. 9. Interestingly, the cation type does not affect the transition pressures very much (see Fig. 10), which can be rationalized as follows: High-pressure phase transitions tend to be largely driven by packing fractions. The main building blocks in our systems are phosphate tetrahedra, which remain stable in the pressure range investigated here[9,12]. As low-coordinated phosphates are networks with a more open structure than the highly-coordinated phosphates, they are softer and have a reduced ability to sustain high pressures without becoming unstable.

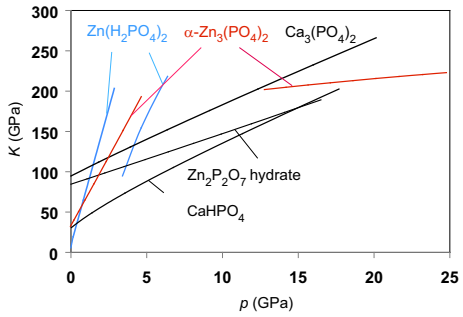

FIG. 9: Bulk modulus as function of pressure during compression of zinc and calcium phosphates. The endpoints of the curves mark the points of amorphization. In the amorphous phase no equation can be obtained. In two cases, however, $Zn(H_2PO_4)_2$ and α-$Zn_3(PO_4)_2$, recrystallization occurs at elevated pressures.

Another interesting observation is that the initial crystalline structures in metal phosphates become unstable when their bulk modulus reaches a value in the vicinity of 210 ± 40 GPa for both high- and low-coordinated metal phosphates. In this context, it is worth recollecting two facts: (a) the bulk modulus is dominated by repulsive interactions, in particular at high pressures (as one can easily ascertain from calculating the bulk modulus of a Lennard Jones system); (b) the softest part in a system (or the weakest repulsion between correlated units) mainly determines the compliance of the system. Given our results, it is thus tempting to speculate that a phosphate network destabilizes when the phosphate units are squeezed into one another so strongly that the bulk modulus of the crystal system that they belong to approaches a value of 210 ± 40 GPa. This speculation is supported

by the observations on the hydrogenated compounds: they have additional compliant sites due to the fact that hydrogen cannot participate in the network formation. Stressing analogies to simple mechanical spring models: the presence of hydrogen makes the whole system become relatively soft, even when the phosphate units are already pushed deeply into their repulsive potentials.

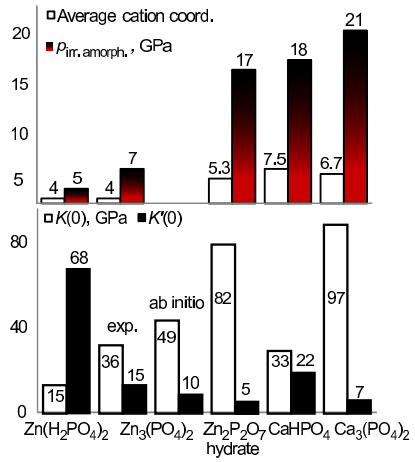

FIG. 10: Summary on the experimental and calculation results. The average coordination of the cation, pressures of the irreversible crystallinity loss $p_{\mathrm{irr.amorph}}$, bulk modulus $K(0)$ and derivative of the bulk modulus $K'(0)$ at ambient conditions.

Open questions are: (i) What modes become unstable as the pressure increases? (ii) Why do the systems amorphize rather than to undergo a displacive phase transition? The *ab initio* simulations presented in this work may give a partial answer to these questions, because detailed structural information can be obtained for systems above their amorphization pressure. In the simulations, the coordination of the cation changes from four to five via a displacive mode of phosphate groups that can be classified as a rigid unit mode[35]. Thus, there should be the possibility for a displacive phase transformation. In fact, in our small simulation cells, we do observe this transformation and it turns out to be reversible. However, in contrast to the experimental structure, the simulated crystal does not contain structural defects such as vacancies, interstitials, and grain boundaries. These can act as nucleation sites for amorphization and prevent recrystallization at large length scales upon decompression.

An important insight from the simulation may be that the high-pressure structure has the higher symmetry, which is in contrast to the frequently observed decrease in symmetry with pressure, see, e.g., the transformation of quartz to quartz II[36], as a prototypical case for a network structure. In the most generic case, any pressure-induced liquid to solid phase transformation can also be seen as a reduction in symmetry from complete isotropy to discrete symmetry. Sometimes, however, symmetry can also increase with pressure, as is the case, for example, in elemental group VI crystals (specifically As, Sb, and Bi)[37]. There, a Peierls-like distortion (PLD)[38] is eliminated through compression. Ultimately, those systems undergo a reconstructive phase transformation, because electrons want to re-open a gap between conduction and valence band. Applying these arguments to the metal phosphate, one could argue that a potential desire to reconstruct is kinetically hindered, which would explain amorphization (also when the reconstruction is not driven by a PLD). However, we believe that the system does not want to reconstruct, because $Zn_3(PO_4)_2$ recrystallizes at very high pressure into a structure which can be reached in principle from the original low-pressure crystal through displacements of PO_4-tetrahedra. Moreover, the crystals reamorphize under decompression and the cations regain their original coordination at low pressures.

While the dramatic stiffening of zinc phosphates may be related to their network character, it is clear that this cannot be the only explanation for the extreme stiffening with pressure. Quartz, a prototypical tetrahedral network, only has a K'(0) ≈ 6,[16] as opposed to our largest value of K'(0) ≈ 60 for $Zn(H_2PO_4)_2$. Part of the difference in the stiffening between those two compounds may be related to the sp^3 hybridization on the silicon atoms in quartz, which may hinder bending to a larger degree than the hybridization on the zinc atom, which involves *d*-electrons. As an alternative explanation, it would be interesting to investigate the idea that the presence of a PLD may be held responsible for the observed effect. Such a study, however, is beyond the scope of the present paper.

B. Tribology

The results obtained on the solid state chemistry of zinc and calcium phosphates presented in this paper, may be useful to rationalize some tribological experiments, which had previously been difficult to explain. Of course, our discussion will be speculative in nature pending further studies. Before providing our interpretation, we would like to remind the reader that lubricating fluids contain a large variety of additives which are each supposed to perform a desired function. Out of the long list of chemicals, there are two additive components which are present in high concentrations, namely antiwear additives and detergents. A common antiwear additive is zinc dialkyldithiophosphate, and a generic detergents is calcium sulfonate. Both function well independently, but in the mixture, their performance is compromised. The antiwear function of ZDDP is related to the formation of a protective layer on the surface consisting mostly of a zinc phosphate glass. The addition of calcium sulfonate results in the formation of a mixed film containing zinc and calcium phosphate[39–41]. Most of the previous studies were focused on investigating the effect of calcium sulfonate on the kinetics of formation of the protective layer, but not on the effect of calcium sulfonate on me-

chanical properties and the response to compression or shear of the protective layer, which may well be related to the changes in the mechanical properties of the films, as we will argue.

We believe that the antiwear function of the film is connected with its sacrificial character[8,42–45]; i.e. the film can be worn off and yet protect the material underneath. In order for this scenario to work, the film has to be softer and have a lower shear strength than the substrate. We believe that the presence of calcium phosphate counteracts this requirement by making the film extraordinarily rigid and firm. This may induce higher wear, because stiff films can mediate higher shear. In this context it can be said that (highly coordinated and thus stiff) calcium phosphates would require a stiffer and harder substrate for them to function successfully as a sacrificial film. From this argument we conclude that it is not necessarily the cation type but the cation coordination or mechanical properties of the phosphate which affect the antiwear action of the protective layer, and it appears as if calcium tends to have high coordination in calcium phosphates, while zinc phosphates in their performance as antiwear agent, are generally assumed to be tetrahedrally coordinated before they arrive at the surface. These arguments are consistent with a recent study[46] in which antiwear and anti-friction properties of phosphates on steel were compared. It was found that low coordinated α-$Zn_3(PO_4)_2$ protect surfaces better and reduce friction as compared to the highly coordinated $Zn_2P_2O_7{\cdot}H_2O$. We would explain these findings within the results of our study, arguing that they are due to the lower yield strength and low initial bulk modulus of the protective α-$Zn_3(PO_4)_2$-containing film. In contrast to the α-$Zn_3(PO_4)_2$ film, $Zn_2P_2O_7{\cdot}H_2O$ preserved its powder morphology and relatively high stiffness under rubbing, acting somewhat abrasive.

Another important quality of the low coordinated zinc phosphates, appears to be their ability to stiffen rapidly under pressure[13]. The origin of this smart material effect can be related to the decrease in the flexibility of rigid unit modes upon compression - with or without change of cation coordination. The stiffening under pressure is particularly strong for hydrogenated metal phosphates. The presence of a hysteresis loop upon compression/decompression cycle might be yet another beneficial feature of zinc phosphates: it can improve the sacrificial character of the film by increasing the dissipation within the film.

Acknowledgments

MHM, YS, and PRN wish to acknowledge support from NSERC and General Motors of Canada Ltd., and MHM from PREA. The research described in this manuscript was performed partially at the National Synchrotron Light Source at Brookhaven National Lab. We acknowledge J.Hu for useful discussions and technical support.

[1] V. F. Buchwald. *Phosphate minerals*. Springer-Verlag, Berlin, 1984.

[2] X. Xie, M. Minitti, M. Chen, H. Mao, D. Wang, J. Shu, and Y. Fei. Natural high-pressure polymorph of merrillite in the shock veins of the Suizhou meteorite. *Geochim. Cosm. Acta*, 66:2439, 2002.

[3] U. Bismayer and W. G. Marshall. Local and long-range order in ferroelastic lead phosphate at high pressure. *Acta crystallographica. Section B, Structural science*, 60:1, 2004.

[4] R. J. Angel, U. Bismayer, and W. G. Marshall. Renormalization of the phase transition in lead phosphate, $Pb_3(PO_4)_2$, by high pressure: structure. *J. Phys.: Condens. Matter*, 13:5353, 2001.

[5] L. Herschke, J. Rottstegge, I. Lieberwirth, and G. Wegner. Zinc phosphate as versatile material for potential biomedical applications part 1. *Journal Of Materials Science: Materials In Medicine*, 17:81, 2006.

[6] E. Fernández, F. J. Gil, S. M. Best, M. P. Ginebra, F. C. M. Driessens, and J. A. Planell. Improvement of the mechanical properties of new calcium phosphate bone cements in the $CaHPO_4$-α-$Ca_3(PO_4)_2$ system: Compressive strength and microstructural development. *Journal of Biomedical Materials Research*, 41(4):560–567, 1998.

[7] L. Tortet, J.R. Gavarri, G. Nihoul, and A.J. Dianoux. Study of protonic mobility in $CaHPO_4{\times}2H_2O$ (Brushite) and $CaHPO_4$(Monetite) by infrared spectroscopy and neutron scattering. *Solid State Ionics*, 97:253, 1997.

[8] M. A. Nicholls, T. Do, P. R. Norton, M. Kasrai, and G. M. Bancroft. Review of the lubrication of metallic surfaces by zinc dialkyl-dithlophosphates. *Tribology International*, 38(1):15–39, 2005.

[9] N. J. Mosey, M. H. Müser, and T. K. Woo. Molecular mechanisms for the functionality of lubricant additives. *Science*, 207:1612, 2005.

[10] N. J. Mosey, T. K. Woo, M. Kasrai, P. R. Norton, G. M. Bancroft, and M. H. Müser. Interpretation of experiments on zddp anti-wear films through pressure-induced cross-linking. *Tribology Letters*, 24:105, 2006.

[11] M. Gauvin, F. Dassenoy, C. Minfray, J. M. Martin, G. Montagnac, and B. Reynard. Zinc phosphate chain length study under high hydrostatic pressure by Raman spectroscopy. *Journal of Applied Physics*, 101:063505, 2007.

[12] D. Shakhvorostov, M. H. Müser, N. J. Mosey, D. J. Munoz-Paniagua, G. Pereira, Y. Song, M. Kasrai, and P. R. Norton. On the pressure-induced loss of crystallinity in orthophosphates of zinc and calcium. *The Journal of Chemical Physics*, 128(7):074706, 2008.

[13] S. Bec, A. Tonck, J. M. Georges, R. C. Coy, J. C. Bell, and G. W. Roper. Relationship between mechanical properties and structures of zinc dithiophosphate anti-wear films. *Proceedings: Mathematical, Physical and Engineering Sciences*, 455:4181–4203, 1999.

[14] K. Takemura and A. Dewaele. Isothermal equation of state

for gold with a He-pressure medium. *Physical Review B*, 78(10), 2008.

[15] G. Misra, P. Tripathi, and S. C. Goyal. Bulk modulus of semiconductors and its pressure derivatives. *Philosophical Magazine Letters*, 87(6):393–401, 2007.

[16] L. G. Liu. Bulk moduli of sio_2 polymorphs - quartz, coesite and stishovite. *Mechanics of Materials*, 14(4):283–290, 1993.

[17] S. N. Vaidya and G. C. Kennedy. Compressibility of 18 metals to 45 kbar. *Journal of Physics and Chemistry of Solids*, 31(10):2329–&, 1970.

[18] S. Raju, E. Mohandas, and V. S. Raghunathan. The pressure derivative of bulk modulus of transition metals: An estimation using the method of model potentials and a study of the systematics. *Journal of Physics and Chemistry of Solids*, 58(9):1367–1373, 1997.

[19] N. J. Mosey, T. K. Woo, and M. H. Müser. *Phys. Rev. B*, 72:054124, 2005.

[20] H. K. Mao, P. M. Bell, J. W. Shaner, and D. J. Steinberg. *Journal of Applied Physics*, 46:543, 1978.

[21] B. M. Nirsha, T. V. Khomutova, A. A. Fakeev, B. V. Zhadanov, V. M. Agre, N. P. Kozlova, and V. A. Olikova. *Russian Journal of Inorganic Chemistry*, 27(5):630, 1982.

[22] R. Car and M. Parrinello. Unified approach for molecular dynamics and density-functional theory. *Phys. Rev. Lett.*, 55:2471, 1985.

[23] J. Hütter, A. Alavi, T. Deutsch, M. Bernasconi, S. Gödecker, D. Marx, M. Tuckerman, and M. Parrinello. *CPMD Version 3.5*. Copyright IBM Zürich Research Laboratory and MPI für Festkörperforschung, 1995-2001.

[24] W. Kohn and L. J. Sham. Self-consistent equations including exchange and correlation effects. *Phys. Rev*, 140A:1133, 1965.

[25] J. P. Perdew, K. Burke, and M. Ernzerhof. Generalized gradient approximation made simple. *Phys. Rev. Lett.*, 77:3865, 1996.

[26] N. Troullier and José Luriaas Martins. Efficient pseudopotentials for plane-wave calculations. *Phys. Rev. B*, 43(3):1993–2006, Jan 1991.

[27] C. Calvo. The crystal structure of α-$Zn_3(PO_4)_2$. *Canadian Journal of Chemistry*, 43(2):436–445, Jul 1965.

[28] Francis Birch. Finite elastic strain of cubic crystals. *Phys. Rev.*, 71(11):809–824, Jun 1947.

[29] N. N. Greenwood and A. Earnshaw. *Chemistry of the elements*. Butterworth-Heinemann, Oxford, 2 edition, 1997.

[30] B. M. Nirsha, T. V. Khomutova, A. A. Fakeev, V.M.Agre, B. V. Zhadanov, G. R. Allakhverdov, N. P. Kozlova, and V. A. Olikova. *Russian Journal of Inorganic Chemistry*, 25(2):213, 1980.

[31] B.E. Robertson and C. Calvo. Crystal structure of α-$Zn_2P_2O_7$. *Journal of Solid State Chemistry*, 1:120–133, 1970.

[32] G. MacLennan and C. A. Beevers. The crystal structure of dicalcium phosphate, $CaHPO_4$. *Acta Crystallographica*, 8(9):579–583, 1955.

[33] W. A. Denne and D. W. Jones. Neutron diffraction investigation of the hydrogen positions in the crystal structure of monetite, $CaHPO_4$. *Journal of Chemical Crystallography*, 1(5):347–354, 1971.

[34] M. Yashima, A. Sakai, T. Kamiyama, and A. Hoshikawa. Crystal structure analysis of β-tricalcium phosphate $Ca_3(PO_4)_2$ by neutron powder diffraction. *Journal of Solid State Chemistry*, 175(2):272–277, November 2003.

[35] K. D. Hammonds, M. T. Dove, A. P. Giddy, V. Heine, and B. Winkler. Rigid-unit phonon modes and structural phase transitions in framework silicates. *American Mineralogist*, 81:1057–1079, 1996.

[36] R. Martonk, D. Donadio, A. R. Oganov, and M. Parrinello. From four- to six-coordinated silica: Transformation pathways from metadynamics. *Physical Review B*, 76:014120, 2007.

[37] O. Degtyareva, M.I. Mcmahon, and R. J. Nelmes. High-pressure structural studies of group-15 elements. *High Pressure Research*, 24:319–356, 2004.

[38] R. E. Peierls. *Quantum theory of solids*. Pergamon, Oxford, 1955.

[39] Z. Yin, M. Kasrai, G. M. Bancroft, K. Fyfe, M. L. Colaianni, and K.H. Tan. *Wear*, 202:194–201, 1997.

[40] M. Kasrai, M. Fuller-Suominen, G. M. Bancroft, and P. R. Ryason. X-ray absorption study of the effect of calcium sulfonate on antiwear film formation generated from neutral and basic zddps: Part 1phosphorus species. *Tribology Transactions*, 46:534 – 542, 2003.

[41] G. Pereira, A. Lachenwitzer, D. Munoz-Paniagua, M. Kasrai, P. R. Norton, T. W. Capehart, T. A. Perry, and Y. T. Cheng. *Tribology Materials, Surfaces & Interfaces*, 1:1, 2007.

[42] F. P. Bowden and D. Tabor. *The Friction and Lubrication of Solids: Part II*. Clarendon Press, Oxford, 1964.

[43] I. V. Kragelsky, M. N. Dobychin, and V. S. Kombalov. *Friction and wear, calculation methods*. Pergamon Press, Oxford, 1982.

[44] J. M. Martin. Antiwear mechanisms of zinc dithiophosphate: a chemical hardness approach. *Tribology Letters*, 6(1):1–8, 1999.

[45] H. Spikes. The history and mechanisms of ZDDP. *Tribology Letters*, 17(3):469–489, 2004.

[46] M. Gauvin, F. Dassenoy, C. Minfray, M. Belin, G. Montagnac, B. Reynard, and J. M. Martin. ZDTP-like antiwear properties of zinc orthophosphate under boundary lubrication. *Annual STLE Meeting, Cleveland, May*, 2008.